Gabrielle Bachand
Department of Materials Science and Engineering,
University of Nevada Reno,
1664 North, Virginia Street,
Reno, NV 89557-0338
e-mail: gbachand@unr.edu

Jason Mennel
Department of Materials Science and Engineering,
University of Nevada Reno,
1664 North, Virginia Street,
Reno, NV 89557-0338
e-mail: jmennel@unr.edu

Dev Chidambaram[1]
Department of Materials Science and Engineering;
Nevada Institute for Sustainability,
University of Nevada Reno,
1664 North, Virginia Street,
Reno, NV 89557-0338
e-mail: dcc@unr.edu

Improved Performance of Silicon Anodes Using Copper Nanoparticles as Additive

Nanoscale copper has been successfully integrated into a silicon-based anode via a cost-effective, one-step process. The additive was found to improve the overall electrical conductivity and charge/discharge cycling performance of the anode. Analysis of the new material shows that copper particles are homogeneously interspersed into the silicon active layer. The formation of Cu_3Si during the annealing step of the fabrication process was also confirmed using X-ray diffraction and is thought to contribute to the structural stability of the anode during cycling. Despite the inclusion of only small quantities of the additive (approximately 3%), anodes with the added copper show significantly higher initial discharge capacity values (957 mAg^{-1}) compared to anodes without copper (309 mAg^{-1}), and they continue to outperform the latter after 100 charge/discharge cycles. Results also show a significant decrease in the resistance of anodes with the additive, a contributing factor in the improvement of the electrochemical performance. [DOI: 10.1115/1.4056841]

Keywords: lithium-ion battery, electrochemical performance, X-ray diffraction, copper silicide, electrochemical storage

Introduction

Development of high capacity yet economically viable Li-ion battery electrode materials remains a high priority in the research field as power demands of new technologies rapidly increase and greater societal concern for the sustainability of materials continues to grow [1]. Restrictions in the performance capabilities of current Li-ion battery materials especially hinder the advancement of electric vehicles, renewable energy generation, and portable technologies [2,3]. One of the most expansively researched anode materials is silicon, and it continues to prove to be a compelling choice compared to other anode candidates due to having the highest theoretical gravimetric capacity of materials for standard Li-ion batteries and exceptional volumetric capacity [4]. Silicon also shines as a sustainable material option due to its general natural abundance and non-toxicity [5]. However, several unfavorable characteristics of silicon prevent the material from becoming more prominently utilized. Factors such as the large volume changes upon lithiation/delithiation and poor capacity retention have hindered the commercial viability of predominantly silicon-based anodes [5–7]. Another prominent issue is the low electrical conductivity of silicon (electron conductivity of 10^{-3} S/cm) compared to that of graphite (10^4 S/cm) [8]. While the low conductivity of silicon is not a significant issue for very thin film electrodes (which almost act as a 2D electrode) for solid-state batteries [9], it needs to be addressed for traditional Li-ion batteries [8]. The most common approach to mitigate this issue is to supplement silicon with a carbon component either in the form of a mixture additive (such as conductive carbon) or as an integrated material. Examples of the latter include carbon-coated silicon [10,11], silicon/carbon embedded frameworks [12], or variations of silicon/carbon composites [13–15]. Literature indicates that additives with higher conductivity provide greater electrical contact within the active material structure, thus enhancing the electrochemical performance of the anode. Though silicon/carbon integration methods have proven successful in demonstrating increased capacity, impressive results have also become achievable with the addition of metallic components.

The addition of different transition metals has been shown to enhance the performance of silicon-based anodes [16–18], and there is significant research investigating silicon/metal composite materials [19]. Many studies have been dedicated to improving silicon anode characteristics, specifically with the addition of copper. Copper is well-known for its high electrical conductivity (resistivity of 1.68×10^{-8} Ωm, 20 °C), and it has been studied in forms such as arrays [20,21], coatings [22,23], and depositions [24,25] with silicon. Silicon/copper composites have been synthesized and yield promising results in improving performance [26–29]. In several reports, Cu_3Si was shown to be an effective contributor to improved stability and performance of silicon anodes as it can have a buffering effect to combat large volume expansion, and the compound can be formed using a variety of facile methods [25,26,30–33]. Copper has also been studied as a nanoparticle additive for anode materials [27,34,35], and it is advantageous that the small particle size allows for thorough integration into the silicon anode structure; however, these studies involve varying degrees of complexity for industry application. Although numerous strategies to help address functional issues with silicon anodes have been explored throughout the past decade, further development of effective and economic solutions is still needed as the demand for improved battery performance continues to grow.

The motivation for this study derives from the concept of using a copper component to lessen the undesirable functional attributes of silicon as an anode, however, accomplishing this by means of a straightforward and economic method. As Li-ion battery fabrication facilities swell in production size, simplicity, and cost-effectiveness of potential solutions are of significant interest and have a greater likelihood of success in the industry [36]. This study investigates the one-step addition of copper nanoparticles via $CuCl_2$ to improve the overall cycling performance of silicon-based anodes. An experimental anode made with $CuCl_2$ as a substitute for conductive carbon is also assessed to determine the viability of using exclusively silicon with $CuCl_2$ as the active material.

Experimental

Sample Preparation. The following chemicals were used for anode fabrication: silicon nanopowder (<100 nm, 98% purity, Sigma-Aldrich), polyvinylpyrrolidone (PVP, Sigma-Aldrich),

[1]Corresponding author.

Manuscript received October 14, 2022; final manuscript received January 31, 2023; published online March 1, 2023. Assoc. Editor: Partha P. Mukherjee.

carbon black Super P (CB, 99% purity, Alfa Aesar), and copper dichloride anhydrous powder (99.995% purity, Beantown Chemical). A control batch was made using approximately 200 mg silicon, 720 mg PVP, and 20 mg CB dissolved in ethanol and mixed to form a homogeneous slurry using a magnetic stirrer at room temperature for 1 h. The control batch was denoted as "Si only." The procedure was replicated for a second batch with the addition of 20 mg copper dichloride, denoted as "Si–Cu." A third batch was then made without CB and with 20 mg copper dichloride, denoted as "Si–Cu (NC)" where "NC" corresponds to "no conductive carbon." Sample procedure as described by Zhong et al. was used to prepare the samples [17].

Two sample preparation methods were executed for physical characterization. Sample slurries were spread onto copper foil using Meyer rod application, and the films were allowed two hours to air-dry prior to annealing under argon at 700 °C for 15 min. Anode discs of 1.3 cm diameter were punched from the annealed foils and were measured to have approximately 0.03 mm thickness and 0.3 mg cm^{-2} material loading.

For further characterization methods, a thin layer of each of the sample slurries was spread on a tantalum foil coupon. Tantalum foil was selected as the platform rather than a copper foil in order to clearly distinguish the copper content in the annealed slurries during characterization methods. The coated coupons were allowed to air-dry for 2 h, and then, they were placed in a tube furnace to anneal under argon at 700 °C for 15 min. Once cooled, the annealed coatings were removed from the tantalum platforms for use in characterization.

For electrochemical testing, annealed and punched anode discs were transferred to an argon-filled glove box for coin cell assembly. The glove box was maintained with water and oxygen at less than 1.0 ppm. The coin cells (CR2032-type) were assembled using 1.3 cm diameter discs of lithium foil (Alfa Aesar, MA, USA) as counter and reference electrode, Celgard 25-μm-thick membrane as separator (MTI), and the experimental anode discs. The electrolyte was a solution of 1.0 M $LiPF_6$ in ethylene carbonate (EC) and diethyl carbonate (DEC) with a 1:1 volume ratio (Sigma-Aldrich). Coin cells were assembled and then sealed with an electric crimper (MTI).

Sample Characterization. The surface characteristics and particle sizing of the anode disc samples were examined using scanning electron microscopy (SEM) with a Hitachi S-4800 microscope (JEOL, Tokyo, Japan). Raman spectroscopy was also performed on the materials using a Thermo Scientific DXR Raman Microscope with a 532-nm laser at 10 mW power. The Raman data were collected at 10× magnification and a spot size of 50 μm. For the remainder of the characterization techniques, annealed coating samples were used. Energy-dispersive X-ray spectroscopy (EDS) was performed on the sample coatings using an Oxford EDS system. The samples were then investigated using X-ray diffraction (XRD) with a Rigaku SmartLab XRD using CuKα radiation from 20 deg to 100 deg 2θ and a step size of 0.07 deg at a scan rate of 0.5 $degmin^{-1}$. Rigaku PDXL2 analysis software and JCPDS cards were used in assessing the XRD data. Following this, inductively coupled plasma optical emission spectrometry (ICP-OES) analysis was conducted using a PerkinElmer ICP-OES 8000 (Waltham, MA) to confirm the presence and composition of copper within the experimental samples. For ICP-OES, samples were dissolved in nitric acid. Calibration standards were purchased from SCP Science, and reported results showed less than 3% relative standard deviation.

Electrochemical Measurement. The fabricated coin cells were then tested using electrochemical impedance spectroscopy (EIS) with an Ametek PARSTAT 4000 instrument and a frequency range from 100 kHz to 0.01 Hz. Then, charge and discharge cycling of the cells was performed using an MTI multichannel battery analyzer, galvanostatically in the voltage range from 0.01 V to 1.5 V at room temperature. To establish active layer lithiation and solid electrolyte interphase (SEI) layer development, cells first completed two cycles at a lower current density of 100 mAg^{-1} before proceeding to full testing. All sample tests were performed at a current density of 250 mAg^{-1} and for 100 cycles.

Results and Discussion

Characterization Results. In producing the anode slurry coatings, homogeneity and even distribution of the copper additive in the mixture is important to maximize the contact of the additive and silicon for greater conductivity. Figures 1(*a*)–1(*c*) show the SEM micrographs of the Si-only, Si–Cu, and Si–Cu (NC) sample surfaces, respectively. As shown, the surfaces are comprised of particles with nanoscale diameters, and the particles form larger aggregates. Particles seen on the anode surface are evaluated to be in the range of 5–20 nm. Little visual difference can be seen between the three samples at 40 k-× magnification, indicating that the addition of $CuCl_2$ did not substantially alter the surface morphology. The particle distribution also appears consistent across the surfaces of the anode discs as there are no anomalous formations. Figures 1(*d*) and 1(*e*) show the results of EDS elemental mapping of copper for the Si–Cu and Si–Cu (NC) samples at 40 k-× magnification, confirming the visual observations that the copper is uniformly distributed throughout the silicon-based coating.

Further SEM analysis, as shown in Fig. 2, illustrates how copper helps improve the conductivity of the electrode. Taken in YAG BSE mode at 1 k-× magnification, clear pathways can be seen of copper particles percolating throughout the surface that would aid in electron transport. Figure 3 shows SEM results contrasting the copper particle sizes compared to silicon and carbon electrode material.

Figure 4 shows a comparison of the Raman spectra of the samples at 10× magnification. All samples exhibit the same four prominent peaks: two corresponding to silicon at approximately 520 cm^{-1} and 950 cm^{-1} [37–40] and two corresponding to graphite carbon [35,41,42]. The graphite D peak and G peak are visible at approximately 1350 cm^{-1} and 1580 cm^{-1} and have similar peak heights between the samples. The calculated intensity ratios for the two carbon peaks (I_D/I_G) of the Si only, Si–Cu, and Si–Cu (NC) are 0.92, 0.96, and 0.95, respectively. The values show the amorphous quality of the carbon in the materials. The prevalence of the amorphous carbon is thought to be derived from the PVP binding material during the annealing step, and groups such as Zhong et al. have shown in previous work that the decomposition of the PVP forms a carbonaceous structure surrounding the other particulates [43]. Though the Si–Cu (NC) sample did not have added carbon in its mixture, the amorphous carbon from the PVP and high weight percentage of PVP used seem sufficiently large to nullify the difference.

The measured amounts of copper present in each sample after the fabrication processes determined by ICP-OES are shown in Table 1. No copper was detected in the control sample. The Si–Cu and Si–Cu (NC) samples contain 3.04% and 2.12% of copper, respectively. Relatively small amounts of the copper additive were used to promote the goal of cost-effectiveness, and smaller quantities of additive metals have been known to have a significant effect on anode performance in previous literature [17,26].

To confirm the presence of copper and to determine the chemistry following the fabrication processes, the samples are analyzed using XRD. The three XRD patterns of the samples are shown in Fig. 5. The peaks for Si are consistent with JCPDS 00-005-0565, and peaks indicating crystalline Cu (JCPDS 00-004-0836) and Cu_3Si (JPCDS 00-059-0262) are well matched with the index. The XRD patterns for Si–Cu and Si–Cu (NC) suggest the formation of the Cu_3Si compound occurred during annealing from the copper additive and is supported in the literature [25,26,44]. Several publications attest to the benefits of Cu_3Si in the anode composition to improve stability [25,30,31] and electrical conductivity [30,44], but the compound does not seem to actively participate during electrochemical reactions with lithium [31,44].

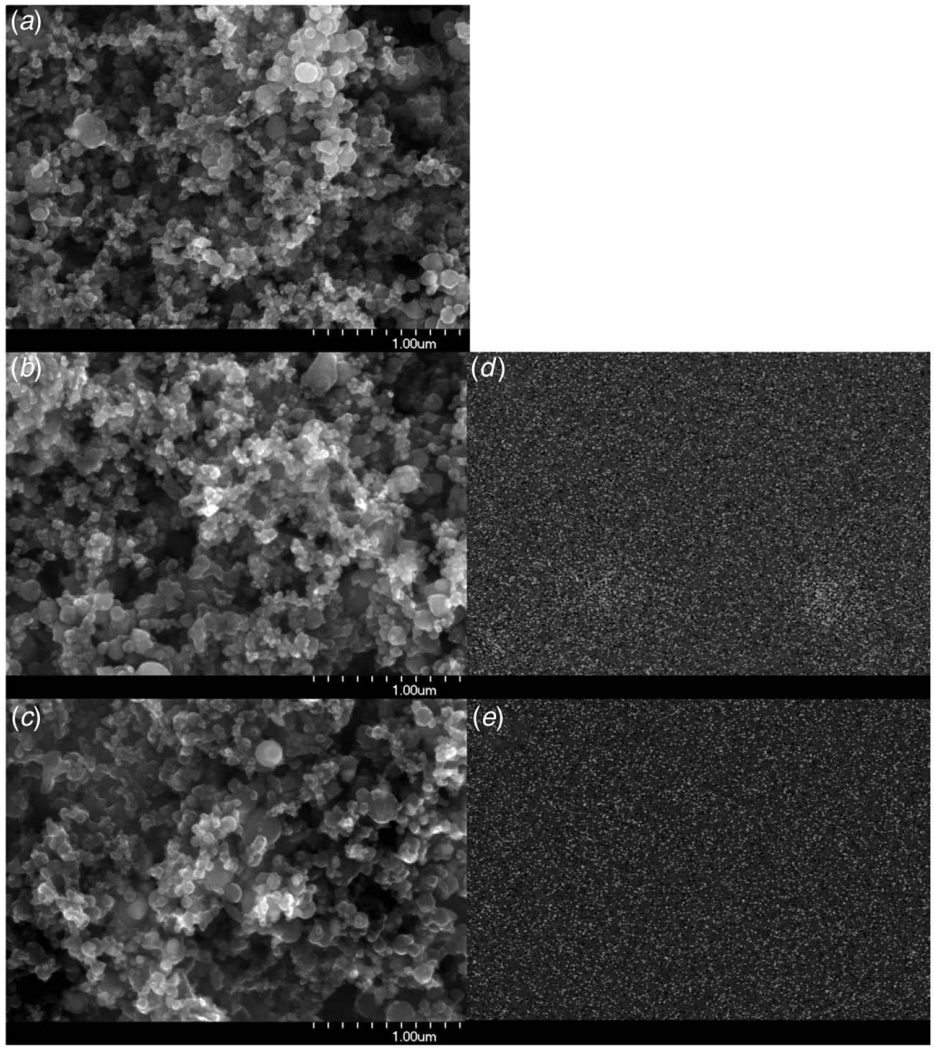

Fig. 1 SEM Images using 20 kV accelerating voltage at 40 k-× magnification of the anode surfaces prior to cycle testing for (*a*) Si only, (*b*) Si–Cu, and (*c*) Si–Cu (NC). The initial surfaces of all three coatings show a similar, homogeneous dispersion of particles with an average size range from 5 nm to 20 nm. EDS elemental mapping of the dispersion of copper is also included in images. (*d*) Si–Cu and (*e*) Si–Cu (NC) at 40 k-× magnification to show the confirmation of the integrated copper nanoparticles. Copper was uniformly distributed in the silicon-based coating.

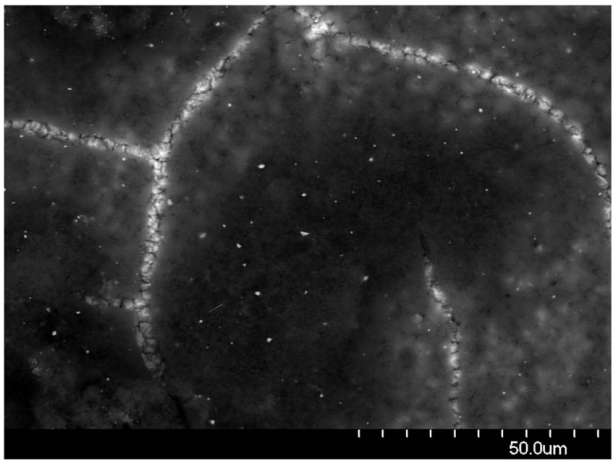

Fig. 2 SEM Image showing Si–Cu anodes at 1 k-× magnification and YAG BSE mode detailing percolating electron-conducting pathways composed of Cu particles

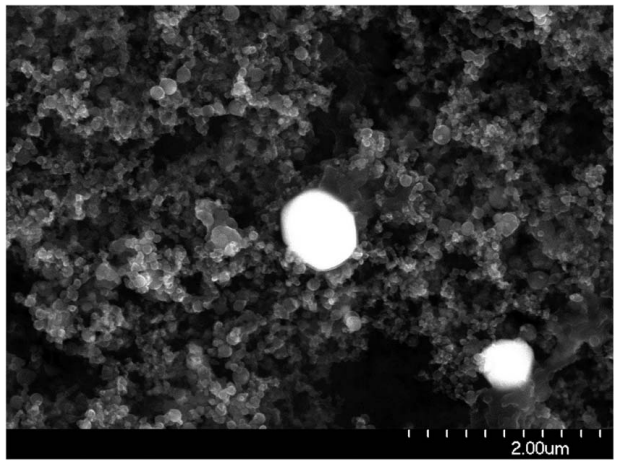

Fig. 3 SEM Image showing the particle sizing of copper compared to the background electrode material at 20 k-× magnification

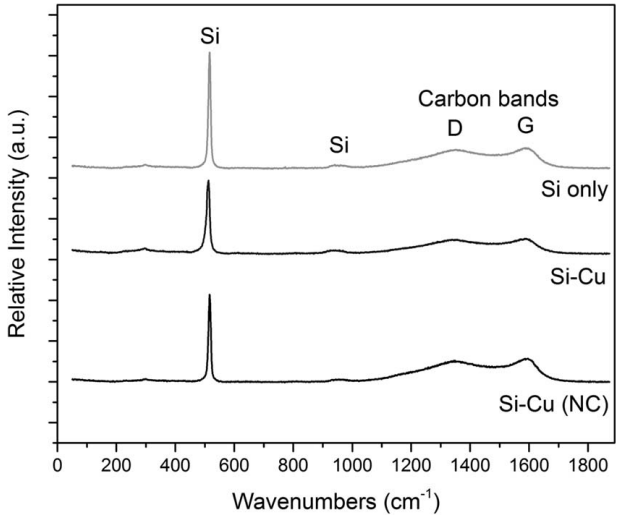

Fig. 4 Raman spectra of the Si-only, Si–Cu, and Si–Cu (NC) coatings at 10× magnification showing the prominent silicon peaks at 520 cm^{-1} and 950 cm^{-1} and the prevalence of the amorphous carbon structure from the two carbon band peaks at 1350 cm^{-1} and 1580 cm^{-1} in each of the three samples

Electrochemical Results. To determine the effects of the copper additive on the anode resistance, the EIS testing shows the comparison of the three samples. The testing is performed prior to any cycle testing of the cells, and the Nyquist plot of the results is shown in Fig. 6. From the plot, two dominant sections of each test are apparent: the semicircle-shaped first portion in the high-to-medium frequency range is attributed to the charge transfer resistance of the anode, and the near linear second portion in the low-frequency range is attributed to the Warburg diffusion element as previously modeled in literature [45,46]. The plot illustrates visible differences in the charge transfer resistances of the samples and confirms that the addition of copper leads to lowered resistivity as seen from the resistance values of 94.04 Ω, 55.39 Ω, and 57.28 Ω for the Si-only, Si–Cu, and Si–Cu (NC) samples, respectively. From the resistance value results, it can be suggested that the copper additive has effectively enhanced the electrical conductivity of the anode.

The cycle testing performance results for each sample are compared in Fig. 7 at a current density of 250 mAg^{-1} for 100 charge/discharge cycles following two cycles at a lowered current density to establish the SEI layer and lithiation of the active material. The current density is calculated to be 0.075 mA/cm^2. As shown in the plot, the first cycle discharge capacities for the samples are 309 mAg^{-1}, 957 mAg^{-1}, and 775 mAg^{-1}, for Si only, Si–Cu, and Si–Cu (NC), respectively. It is well known that the Si anode undergoes extreme volume expansion in the first few cycles. This causes the SEI to crack significantly, needing to re-form every cycle and incorporate more lithium. The low capacity of the first cycle shows that just silicon alone cannot form a strong, stable, and low resistive SEI for facile lithium-ion transport. Coulombic efficiencies of the anodes also show the relative stability of all three samples; though samples with copper additive display greater variations in efficiency, deviations remain less than 2% of the Si-only sample. Si–Cu and Si–Cu (NC) sample coulombic

Table 1 Measured copper content from ICP analysis for the Si-only, Si–Cu, and Si–Cu (NC) composites

	Si only	Si–Cu	Si–Cu (NC)
Cu Content (%)	0.00	3.04	2.12

Note: The results confirm the quantity of the copper additive.

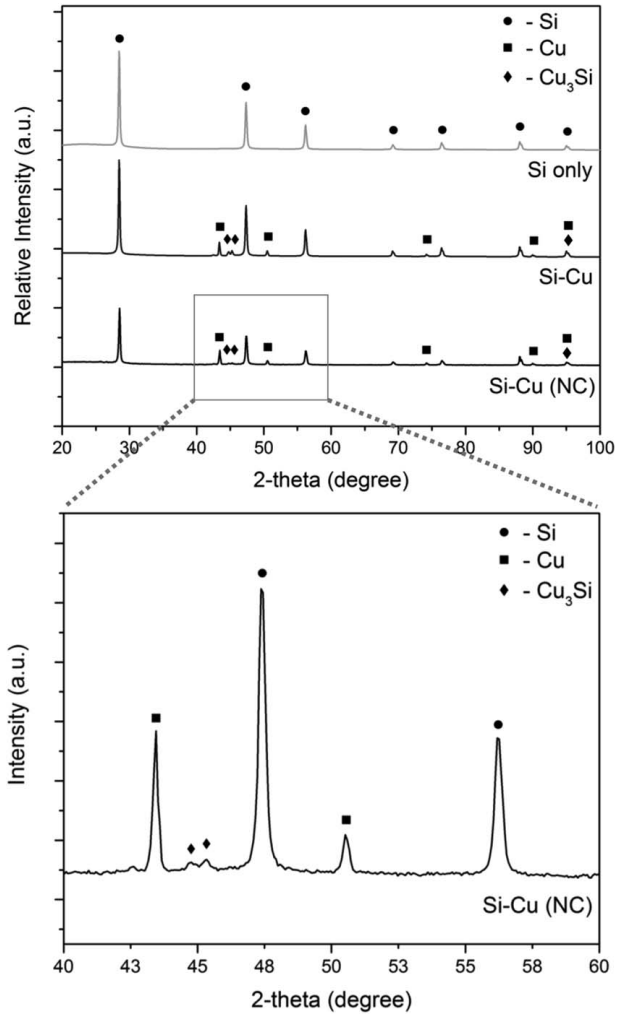

Fig. 5 XRD Patterns of the Si-only, Si–Cu, and Si–Cu (NC) composite materials show the presence of copper and the formation of Cu_3Si in both Si–Cu and Si–Cu (NC)

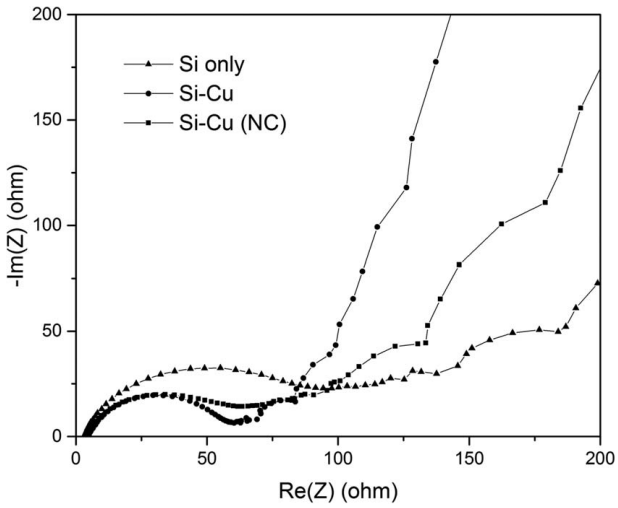

Fig. 6 EIS Curves of the experimental data for the sample anodes prior to cycle testing. Resistance values are 94.04 Ω, 55.39 Ω, and 57.28 Ω for the Si-only, Si–Cu, and Si–Cu (NC) samples, respectively. Thus, the addition of copper leads to increased conductivity in anodes.

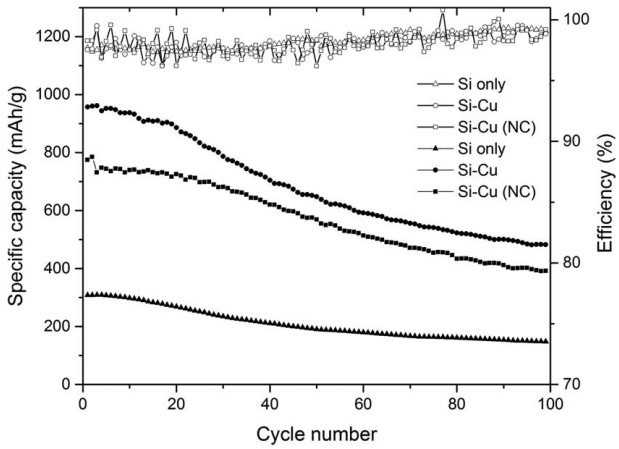

Fig. 7 Capacity and efficiency of the cells as a function of cycle number for the Si-only, Si–Cu, and Si–Cu (NC) anodes cycled at 250 mA g^{-1} current density. Anodes with the incorporated $CuCl_2$ showed increased capacity for the duration of 100 cycles and reasonable stability in efficiency.

efficiencies are also consistently greater than 96%, reaching over 99% efficiency in the final testing cycles. The discharge capacities for the one-hundredth cycle are 148 mAg^{-1}, 482 mAg^{-1}, and 391 mAg^{-1}, for Si only, Si–Cu, and Si–Cu (NC), respectively. After 100 cycles, both anodes with copper additive retain over twice the capacity of the Si-only anode. From these results, it can be seen that even small quantities of copper additive dispersed in the anode structure have a noteworthy effect on the cycling performance of the anode.

Discussion

The results of this work provide further support that copper can serve as an effective conductive additive to silicon anodes, and the one-step method of adding copper to the silicon structure is advantageous in comparison to reports detailing cost-intensive, complex processes. The work joins others with similar goals of simplifying the fabrication process and improving the performance of silicon-based anodes. One such study by Zhong et al. demonstrates similar increased specific capacity and material conductivity results for silicon anodes with tin additive [17]. Though the anodes with tin additive experience a reduction in measured resistivity of over 50% in the study, tin is known to have a lower conductivity (resistivity of 1.09×10^{-7} Ωm, 20 °C) than copper. Resistivity of the anodes with copper, as shown in Fig. 6, is reduced by over 40%, but resistivity values are overall significantly lower than those documented by Zhong et al. Both this study and that of Zhong et al. show that the additives enable improved cycling results for anodes when compared to control samples. Many studies have also been conducted using a combination of tin and copper in primarily composite or alloy form but not in a similar capacity to the methodology of this report with a silicon-based anode, indicating a possible route for future studies [47–54].

Also in pursuit of a less resource-intensive route to form a copper-incorporated silicon anode, the work performed by Cheng et al. describes the addition of copper acetate in a silicon-based mixture to form silicon/carbon/copper composite materials [26]. Characterization of these materials provides confirmation of Cu_3Si formation following the annealing step, and anodes with reported 2.2 weight % of copper content from ICP analysis yield a high average specific capacity of 990 mAh g^{-1} at 200 mA g^{-1} current density during cycle testing. Cycle testing results included in Fig. 7 show comparable specific capacity values, though fewer precursor materials and fabrication steps were required to obtain these results. Figure 8 illustrates the discharge behavior of the cell for all the samples at their first and hundredth cycles. These

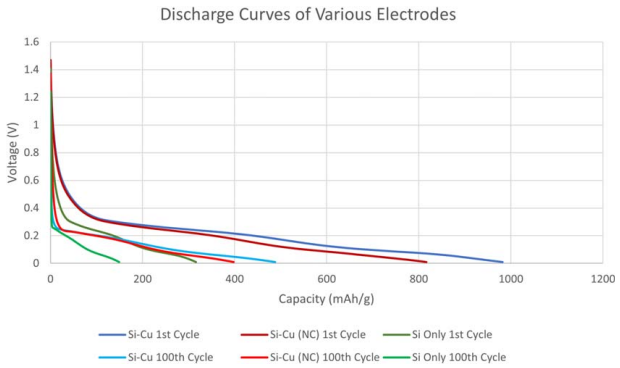

Fig. 8 Discharge curves of the three silicon samples at the first and hundredth cycles. The Si–Cu electrode curves are shown in blue, the Si–Cu (NC) curves shown in red, and the silicon-only control shown in green.

discharge curves reflect lithium leaving the metal electrode and intercalating into the silicon electrode. Figure 9 shows the charging behavior of the cell again for all samples at their first and hundredth cycles. The charge curves are reflective of lithium de-intercalating from the silicon anode to migrate toward the lithium metal. One can easily see the benefit of having carbon black within the electrode, and the superior performance of both to just silicon. This work also differs from common previous studies in showing the characterization of the materials when "battery-ready" or immediately before use in electrochemical tests. This method ensures that any participation of the binder, CB, or final fabrication steps is included in all analyses. Comparable to Zhong et al.'s, this study also explores the substitution of CB with the conductive additive, further reducing the number of necessary materials in the anode mixture and thereby enabling increased silicon content [17].

The work by Fang et al. also demonstrates a one-step process of directly adding copper nanoparticles to a standard silicon slurry; however, the anodes suffer from poor capacity retentions of under 45% for all samples with the copper additive during cycle testing [27]. Despite this, further tests of these samples reinforce the assertion that copper additives increase the conductivity of the anode material and do provide a performance improvement over a purely silicon-based control as also confirmed by this report. A previous study conducted by Kim et al. also explores using specifically $CuCl_2$ as a precursor material in a silicon-based mixture, but the $CuCl_2$-to-Si ratio is 2.683:1 [44]. An initial discharge capacity of 680 mAh g^{-1} is achieved for the material during cycle testing at a constant current of 50 mAh g^{-1} [44]. Though cycle testing at five

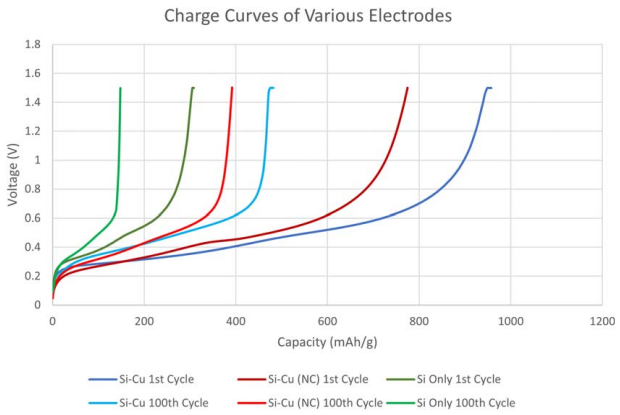

Fig. 9 Charge curves of the three silicon samples at the first and hundredth cycles. The Si–Cu electrode curves are shown in blue, the Si–Cu (NC) curves shown in red, and the silicon-only control shown in green.

times the current rate of the aforementioned anodes, anodes in this report achieve a higher initial discharge capacity (957 mAg^{-1}) with a significantly smaller quantity of the added copper material (3%) and fewer fabrication steps.

In summary, this study supports the collective works that demonstrate how the addition of copper can enhance the performance of silicon anodes. Cycling results for these anodes are comparable with those of similar studies with copper-integrated silicon particles, and the reduction of resistivity of the anodes is also exhibited [23,26,27]. The highlight of this research is the facile fabrication process employed with its proximity to current industry practices.

Conclusions

This report shows the successful fabrication of silicon-based anodes with copper additive, and the results of electrochemical testing show that anodes with the additive have significantly improved performance characteristics. Using off-the-shelf anhydrous $CuCl_2$ powder, copper particles are introduced to the silicon-based slurry and are homogeneously dispersed within the anode structure. Characterization of the anode shows the formation of copper nanoparticles and Cu_3Si within the silicon structure. Cycle testing data show that anodes prepared with the copper additive have increased discharge capacities of over 200% compared to anodes without copper, and high efficiencies of over 96% are achieved. The addition of copper also yields an improvement in the anode conductivity, contributing to the more effective utilization of the active layer composition and thus enabling higher cycling performance. Anodes prepared using the copper additive as a replacement for the traditionally used conductive carbon also show superior performance in comparison to control samples. Thus, it is demonstrable that the copper additive is capable of improving anode cycling behavior in place of conductive carbon to decrease the electrical resistivity of the anode. This research offers a potential economic, straightforward method for improving silicon anode performance although further research is necessary to form silicon anodes with cycling lifetimes comparable to commercial Li-ion battery anodes.

Acknowledgment

This research infrastructure was partially supported by the Office of Vice President for Research Innovation at the University of Nevada, Reno via an AIRE Grant. This work was partly funded by the National Aeronautics and Space Administration under award 80NSSC19M0152. Dr. Ali Shaykhian serves as the NASA technical monitor. Characterization of electrodes was conducted at Materials Characterization Nevada, a user facility at UNR.

Conflict of Interest

There are no conflicts of interest.

Data Availability Statement

The data sets generated and supporting the findings of this article are obtainable from the corresponding author upon reasonable request.

References

[1] Armand, M., and Tarascon, J. M., 2008, "Building Better Batteries," Nature, **451**(7179), pp. 652–657.
[2] Blomgren, G. E., 2017, "The Development and Future of Lithium Ion Batteries," J. Electrochem. Soc., **164**(1), pp. A5019–A5025.
[3] Suciu, G., and Pasat, A., 2017, "Challenges and Opportunities for Batteries of Electric Vehicles," Proceedings of the 2017 10th International Symposium on Advanced Topics in Electrical Engineering (ATEE), Bucharest, Romania, Mar. 23–25, IEEE, pp. 113–117.
[4] Beattie, S. D., Larcher, D., Morcrette, M., Simon, B., and Tarascon, J. M., 2008, "Si Electrodes for Li-Ion Batteries—A New Way to Look at an Old Problem," J. Electrochem. Soc., **155**(2), pp. A158–A163.
[5] Su, X., Wu, Q. L., Li, J. C., Xiao, X. C., Lott, A., Lu, W. Q., Sheldon, B. W., and Wu, J., 2014, "Silicon-Based Nanomaterials for Lithium-Ion Batteries: A Review," Adv. Energy Mater., **4**(1), p. 23.
[6] Beaulieu, L. Y., Hatchard, T. D., Bonakdarpour, A., Fleischauer, M. D., and Dahn, J. R., 2003, "Reaction of Li with Alloy Thin Films Studied by in Situ AFM," J. Electrochem. Soc., **150**(11), pp. A1457–A1464.
[7] Baker, D. R., Verbrugge, M. W., and Bower, A. F., 2016, "Swelling and Elastic Deformation of Lithium-Silicon Electrode Materials," J. Electrochem. Soc., **163**(5), pp. A624–A631.
[8] Zhang, C., Wang, F., Han, J., Bai, S., Tan, J., Liu, J., and Li, F., 2021, "Challenges and Recent Progress on Silicon-Based Anode Materials for Next-Generation Lithium-Ion Batteries," Small Struct., **2**(6), p. 2100009.
[9] Tan, D. H. S., Chen, Y.-T., Yang, H., Bao, W., Sreenarayanan, B., Doux, J.-M., Li, W., et al., 2021, "Carbon-Free High-Loading Silicon Anodes Enabled by Sulfide Solid Electrolytes," Science, **373**(6562), pp. 1494–1499.
[10] Ng, S. H., Wang, J. Z., Wexler, D., Konstantinov, K., Guo, Z. P., and Liu, H. K., 2006, "Highly Reversible Lithium Storage in Spheroidal Carbon-Coated Silicon Nanocomposites as Anodes for Lithium-Ion Batteries," Angew. Chem.-Int. Edit., **45**(41), pp. 6896–6899.
[11] Yoo, J. K., Kim, J., Jung, Y. S., and Kang, K., 2012, "Scalable Fabrication of Silicon Nanotubes and Their Application to Energy Storage," Adv. Mater., **24**(40), pp. 5452–5456.
[12] Zhang, R. Y., Du, Y. J., Li, D., Shen, D. K., Yang, J. P., Guo, Z. P., Liu, H. K., Elzatahry, A. A., and Zhao, D. Y., 2014, "Highly Reversible and Large Lithium Storage in Mesoporous Si/C Nanocomposite Anodes With Silicon Nanoparticles Embedded in a Carbon Framework," Adv. Mater., **26**(39), pp. 6749–6755.
[13] Sourice, J., Bordes, A., Boulineau, A., Alper, J. P., Franger, S., Quinsac, A., Habert, A., et al.et al., 2016, "Core-Shell Amorphous Silicon-Carbon Nanoparticles for High Performance Anodes in Lithium Ion Batteries," J. Power Sources, **328**, pp. 527–535.
[14] Tocoglu, U., Cevher, O., Cetinkaya, T., Guler, M. O., and Akbulut, H., 2014, "Cyclic Performance Study of Silicon/Carbon Nanotube Composite Anodes Using Electrochemical Impedance Spectroscopy," Acta Phys. Pol. A, **125**(2), pp. 290–292.
[15] Wang, C. S., Wu, G. T., Zhang, X. B., Qi, Z. F., and Li, W. Z., 1998, "Lithium Insertion in Carbon-Silicon Composite Materials Produced by Mechanical Milling," J. Electrochem. Soc., **145**(8), pp. 2751–2758.
[16] Yang, X. L., Wen, Z. Y., Huang, S. H., Zhu, X. J., and Zhang, X. F., 2006, "Electrochemical Performances of Silicon Electrode With Silver Additives," Solid State Ion., **177**(26–32), pp. 2807–2810.
[17] Zhong, L., Beaudette, C., Guo, J., Bozhilov, K., and Mangolini, L., 2016, "Tin Nanoparticles as an Effective Conductive Additive in Silicon Anodes," Sci. Rep., **6**(1), pp. 1–8.
[18] Chan, C. K., Zhang, X. F., and Cui, Y., 2008, "High Capacity Li ion Battery Anodes Using Ge Nanowires," Nano Lett., **8**(1), pp. 307–309.
[19] Liang, B., Liu, Y. P., and Xu, Y. H., 2014, "Silicon-based Materials as High Capacity Anodes for Next Generation Lithium ion Batteries," J. Power Sources, **267**, pp. 469–490.
[20] Guan, H., Wang, X., Chen, S. M., Bando, Y., and Golberg, D., 2011, "Coaxial Cu-Si@C Array Electrodes for High-Performance Lithium ion Batteries," Chem. Commun., **47**(44), pp. 12098–12100.
[21] Wang, N., Hang, T., Zhang, W. J., and Li, M., 2016, "Highly Conductive Cu Nanoneedle-Array Supported Silicon Film for High-Performance Lithium Ion Battery Anodes," J. Electrochem. Soc., **163**(3), pp. A380–A384.
[22] Chen, H. X., Xiao, Y., Wang, L., and Yang, Y., 2011, "Silicon Nanowires Coated With Copper Layer as Anode Materials for Lithium-Ion Batteries," J. Power Sources, **196**(16), pp. 6657–6662.
[23] Murugesan, S., Harris, J. T., Korgel, B. A., and Stevenson, K. J., 2012, "Copper-Coated Amorphous Silicon Particles as an Anode Material for Lithium-Ion Batteries," Chem. Mater., **24**(7), pp. 1306–1315.
[24] Polat, B. D., and Keles, O., 2015, "Improving Si Anode Performance by Forming Copper Capped Copper-Silicon Thin Film Anodes for Rechargeable Lithium Ion Batteries," Electrochim. Acta, **170**, pp. 63–71.
[25] Kim, J. W., Ryu, J. H., Lee, K. T., and Oh, S. M., 2005, "Improvement of Silicon Powder Negative Electrodes by Copper Electroless Deposition for Lithium Secondary Batteries," J. Power Sources, **147**(1–2), pp. 227–233.
[26] Cheng, Y., Yi, Z., Wang, C. L., Wang, L. D., Wu, Y. M., and Wang, L. M., 2016, "Influence of Copper Addition for Silicon-Carbon Composite as Anode Materials for Lithium Ion Batteries," RSC Adv., **6**(8), pp. S6756–S6764.
[27] Fang, K., Wang, M., Xia, Y., Li, J., Ji, Q., Yin, S., Xie, S., et al.et al., 2017, "Facile Fabrication Of Silicon Nanoparticle Lithium-Ion Battery Anode Reinforced With Copper Nanoparticles," Dig. J. Nanomater. Biostruct., **12**(2), pp. 243–253.
[28] Xu, K. Q., Zhang, Z. Z., Su, W., and Huang, X. J., 2017, "Core-Shell Si/Cu Nanocomposites Synthesized by Self-Limiting Surface Reaction as Anodes for Lithium Ion Batteries," Funct. Mater. Lett., **10**(3), p. 1750025.
[29] Ling, L., Ma, Y. T., Xie, Q. S., Wang, L. S., Zhang, Q. F., and Peng, D. L., 2017, "Copper-Nanoparticle-Induced Porous Si/Cu Composite Films as an Anode for Lithium Ion Batteries," ACS Nano, **11**(7), pp. 6893–6903.

[30] Kim, S. O., and Manthiram, A., 2016, "Low-Cost Carbon-Coated Si-Cu3Si-Al2O3 Nanocomposite Anodes for High-Performance Lithium-Ion Batteries," J. Power Sources, **332**, pp. 222–229.
[31] Woo, J. Y., Kim, A. Y., Kim, M. K., Lee, S. H., Sun, Y. K., Liu, G. C., and Lee, J. K., 2017, "Cu3Si-Doped Porous-Silicon Particles Prepared by Simplified Chemical Vapor Deposition Method as Anode Material for High-Rate and Long Cycle Lithium-Ion Batteries," J. Alloy. Compd., **701**, pp. 425–432.
[32] Yoon, S., Lee, S. I., Kim, H., and Sohn, H. J., 2006, "Enhancement of Capacity of Carbon-Coated Si-Cu3Si Composite Anode Using Metal-Organic Compound for Lithium-ion Batteries," J. Power Sources, **161**(2), pp. 1319–1323.
[33] Zhou, J. B., Lin, N., Han, Y., Zhou, J., Zhu, Y. C., Du, J., and Qian, Y. T., 2015, "Cu3Si@Si Core-Shell Nanoparticles Synthesized Using a Solid-State Reaction and Their Performance as Anode Materials for Lithium ion Batteries," Nanoscale, **7**(37), pp. 15075–15079.
[34] Jeong, M., Ahn, S., Yokoshima, T., Nara, H., Momma, T., and Osaka, T., 2016, "New Approach for Enhancing Electrical Conductivity of Electrodeposited Si-Based Anode Material for Li Secondary Batteries: Self-Incorporation of Nano Cu Metal in Si-O-C Composite," Nano Energy, **28**, pp. 51–62.
[35] Han, P., Yuan, T., Yao, L., Han, Z., Yang, J. H., and Zheng, S. Y., 2016, "Copper Nanoparticle-Incorporated Carbon Fibers as Free-Standing Anodes for Lithium-Ion Batteries," Nanoscale Res. Lett., **11**(1).
[36] Gauthier, M., Mazouzi, D., Reyter, D., Lestriez, B., Moreau, P., Guyomard, D., and Roue, L., 2013, "A Low-Cost and High Performance Ball-Milled Si-Based Negative Electrode for High-Energy Li-Ion Batteries," Energy Environ. Sci., **6**(7), pp. 2145–2155.
[37] Nadimpalli, S. P. V., Sethuraman, V. A., Dalavi, S., Lucht, B., Chon, M. J., Shenoy, V. B., and Guduru, P. R., 2012, "Quantifying Capacity Loss due to Solid-Electrolyte-Interphase Layer Formation on Silicon Negative Electrodes in Lithium-Ion Batteries," J. Power Sources, **215**, pp. 145–151.
[38] Sethuraman, V. A., Srinivasan, V., and Newman, J., 2013, "Analysis of Electrochemical Lithiation and Delithiation Kinetics in Silicon," J. Electrochem. Soc., **160**(2), pp. A394–A403.
[39] Uchinokura, K., Sekine, T., and Matsuura, E., 1972, "Raman Scattering By Silicon," Solid State Commun., **11**(1), pp. 47–49.
[40] Parker, J. H., Feldman, D. W., and Ashkin, M., 1967, "Raman Scattering By Silicon And Germanium," Phys. Rev., **155**(3), pp. 712–714.
[41] Kim, H., Hwang, T., Kang, K., Pichler-Nagl, J., So, D. S., Park, S., and Huh, H., 2017, "Preparation of Silicon Nanoball Encapsulated With Graphene Shell by CVD and Electroless Plating Process," J. Ind. Eng. Chem., **50**, pp. 115–122.
[42] Wang, C., Luo, F., Lu, H., Rong, X. H., Liu, B. N., Chu, G., Sun, Y., et al., 2017, "A Well-Defined Silicon Nanocone-Carbon Structure for Demonstrating Exclusive Influences of Carbon Coating on Silicon Anode of Lithium-Ion Batteries," ACS Appl. Mater. Interfaces, **9**(3), pp. 2806–2814.
[43] Zhong, L. L., Guo, J. C., and Mangolini, L., 2015, "A Stable Silicon Anode Based on the Uniform Dispersion of Quantum Dots in a Polymer Matrix," J. Power Sources, **273**, pp. 638–644.
[44] Kim, J. H., Kim, H., and Sohn, H. J., 2005, "Addition of Cu for Carbon Coated Si-Based Composites as Anode Materials for Lithium-Ion Batteries," Electrochem. Commun., **7**(5), pp. 557–561.
[45] Guo, J. C., Sun, A., Chen, X. L., Wang, C. S., and Manivannan, A., 2011, "Cyclability Study of Silicon-Carbon Composite Anodes for Lithium-Ion Batteries Using Electrochemical Impedance Spectroscopy," Electrochim. Acta, **56**(11), pp. 3981–3987.
[46] Sharma, N., Plevert, J., Rao, G. V. S., Chowdari, B. V. R., and White, T. J., 2005, "Tin Oxides With Hollandite Structure as Anodes for Lithium Ion Batteries," Chem. Mater., **17**(18), pp. 4700–4710.
[47] Chen, J. Z., Yang, L., Fang, S. H., Hirano, S., and Tachibana, K., 2012, "Three-Dimensional Core-Shell Cu@Cu6Sn5 Nanowires as the Anode Material for Lithium Ion Batteries," J. Power Sources, **199**, pp. 341–345.
[48] Fan, X., Tang, X. N., Ma, D. Q., Bi, P., Jiang, A. N., Zhu, J., and Xu, X. H., 2014, "Novel Hollow Sn-Cu Composite Nanoparticles Anodes for Li-Ion Batteries Prepared by Galvanic Replacement Reaction," J. Solid State Electrochem., **18**(4), pp. 1137–1145.
[49] Kim, J. C., and Kim, D. W., 2014, "Electrospun Cu/Sn/C Nanocomposite Fiber Anodes With Superior Usable Lifetime for Lithium- and Sodium-Ion Batteries," Chem.-Asian J., **9**(11), pp. 3313–3318.
[50] Lin, Y. M., Abel, P. R., Gupta, A., Goodenough, J. B., Heller, A., and Mullins, C. B., 2013, "Sn-Cu Nanocomposite Anodes for Rechargeable Sodium-Ion Batteries," ACS Appl. Mater. Interfaces, **5**(17), pp. 8273–8277.
[51] Liu, S., Li, Q., Chen, Y. X., and Zhang, F. J., 2009, "Carbon-coated Copper-Tin Alloy Anode Material for Lithium Ion Batteries," J. Alloy. Compd., **478**(1–2), pp. 694–698.
[52] Ren, J. G., He, X. M., Wang, L., Pu, W. H., Jiang, C. Y., and Wan, C. R., 2007, "Nanometer Copper-Tin Alloy Anode Material for Lithium-Ion Batteries," Electrochim. Acta, **52**(7), pp. 2447–2452.
[53] Xue, L. G., Fu, Z. H., Yao, Y., Huang, T., and Yu, A. S., 2010, "Three-Dimensional Porous Sn-Cu Alloy Anode for Lithium-Ion Batteries," Electrochim. Acta, **55**(24), pp. 7310–7314.
[54] Zhao, X. Y., Xia, Z. H., and Xia, D. G., 2010, "Electrochemical Performance of Sn Film Reinforced by Cu Nanowire," Electrochim. Acta, **55**(20), pp. 6004–6009.